Chin. Geogra. Sci. 2018 Vol. 28 No. 5 pp. 773–783
https://doi.org/10.1007/s11769-018-0968-0

Springer Science Press
www.springerlink.com/content/1002-0063

Extreme Flood Events over the Past 300 Years Inferred from Lake Sedimentary Grain Sizes in the Altay Mountains, Northwestern China

ZHOU Jianchao[1,2], WU Jinglu[1,3], ZENG Haiao[1]

(1. *State Key Laboratory of Lake Science and Environment*, *Nanjing Institute of Geography and Limnology*, *Chinese Academy of Sciences*, *Nanjing* 210008, *China*; 2. *University of Chinese Academy of Sciences*, *Beijing* 100049, *China*; 3. *Research Center for Ecology and Environment of Central Asia*, *Chinese Academy of Sciences*, *Ürümqi* 830011, *China*)

Abstract: Understanding the temporal variations of extreme floods that occur in response to climate change is essential to anticipate the trends in flood magnitude and frequency in the context of global warming. However, long-term records of paleofloods in arid regions are scarce, thus preventing a thorough understanding of such events. In this study, a reconstruction of paleofloods over the past 300 years was conducted through an analysis of grain sizes from the sediments of Kanas Lake in the Altay Mountains of northwestern China. Results showed that grain parameters and frequency distributions can be used to infer possible abrupt environmental events within the lake sedimentary sequence, and two extreme flood events corresponding to ca. 1736–1765 AD and ca. 1890 AD were further identified based on canonical discriminant analysis (CDA) and coarse percentile versus median grain size (C-M) pattern analysis, both of which occurred during warmer and wetter climate conditions by referring to tree-ring records. These two flood events are also evidenced by lake sedimentary records in the Altay and Tianshan mountains. Furthermore, through a comparison with other records, the flood event from ca. 1736–1765 AD in the study region seems to have occurred in both the arid central Asia and the Alps in Europe, and thus may have been associated with changes in the North Atlantic Oscillation (NAO) index.

Keywords: flood events; grain size; Kanas Lake; Altay Mountains; North Atlantic Oscillation (NAO)

Citation: ZHOU Jianchao, WU Jinglu, ZENG Haiao, 2018. Extreme Flood Events over the Past 300 Years Inferred from Lake Sedimentary Grain Sizes in the Altay Mountains, Northwestern China. *Chinese Geographical Science*, 28(5): 773–783. https://doi.org/10.1007/s11769-018-0968-0

1 Introduction

Global climate change has the potential to accelerate the hydrological cycle, which may further enhance the temporal frequency of regional extreme floods (Pall et al., 2011; Li et al., 2013). Substantial attention has been paid to extreme floods as a consequence of the worldwide increase of their magnitude and frequency (Easterling et al., 2000; Min et al., 2011). Pertinent observations reveal an increased intensity of hydrological extremes at mid and high latitudes (Liu and Zipser, 2015), and climatic models predict that intra-annual rainfall variability will intensify, which will shift current rainfall regimes towards more extreme systems with lower precipitation frequencies, longer dry periods, and larger individual precipitation events worldwide (IPCC, 2013). Therefore, an improved understanding of past observed and future expected extreme flooding is critically necessary.

Arid regions are predicted to be among the ecosystems most affected by climate and environmental changes (Wang et al., 2016). Previous studies have

Received date: 2017-05-12; accepted date: 2017-09-05
Foundation item: Under the auspices of National Key Research and Development Program of China (No. 2017YFA0603400), National Science Foundation of China (No. 41671200, U1603242)
Corresponding author: WU Jinglu. E-mail: w.jinglu@niglas.ac.cn

shown that sedimentary records from arid central Asia (ACA) demonstrated the most sensitivity to hydrological changes during the past millennium (Chen et al., 2015). Coincident with the shift from warm and dry conditions to a warm and humid regime during the late 1980s in northwest China (Shi et al., 2003; 2007), the uncertainty of surrounding potential precipitation increased, and the frequency of large floods caused by heavy rainfalls and rapid snowmelt also increased (Zhang et al., 2017), which wreaked numerous detrimental effects on regional economic and social development. Accordingly, more reliable paleoflood records need to be established for arid regions in order to understand the occurrence of severe floods. Since currently available instrumental data are not long enough for capturing the most extreme events, the acquisition of long duration datasets for historical floods that extend beyond available instrumental records is clearly an important step in discerning trends in flood frequency and magnitude with respect to climate change. Lakes act as efficient repositories for clastic materials that have been eroded from catchment areas and subsequently experienced transport by a fluvial system (Oldfield, 2005). Lake sediments have been proven to be a valuable archive of recurrence rates and intensities of past floods, as they constitute a natural sink for sediments transported by run-off (Corella et al., 2014).

Grain-size in lake sediments has been widely employed as a proxy for past environmental conditions because it is sensitive to climate change and is unaffected by biological activity (Chen et al., 2004; Xiao et al., 2009; Ma et al., 2015). Hydrodynamic relationships represent interaction between the entrainment potential of specific grain sizes and river discharge, which is reflected in the materials received by the lake basin and incorporated into the sediment record, high magnitude flows should appear as distinct laminations of coarse material (Schillereff et al., 2014). As a result, a growing number of palaeolimnologists are searching for lake sediment sequences with which to reconstruct paleoflood records by utilizing grain-size parameters (Wihelm et al., 2012; Amann et al., 2015).

In an attempt to investigate the climate conditions and controlling factors of flood events in arid region, in the current study, an examination of a well-dated sediment core from Kanas Lake of Xinjiang Uygur Autonomous Region was conducted by using grain-size parameters, including grain size distribution, standard deviation, kurtosis, skewness and frequency distribution curves. Our aim is to reconstruct a 300-year flood history in the Altay mountains, expand our knowledge of characters of extreme flood events in high mountains in arid region, and enhance our understanding of the occurrence of severe floods in this region in the context of global warming.

2 Materials and Methods

2.1 Study Area

Kanas Lake (48°42′–48°53′N, 86°59′–87°09′E, 1362 m a.s.l) is an alpine lake located in the southwestern Altay Mountains of northwestern China. The lake extends approximately 24.0 km in a northeast-southwest direction and only 2.6 km in an east-west direction (Fig. 1). It has an area of 45 km^2 with an average water depth of 97 m and a maximum depth of 197 m. The present-day lake water possesses an average salinity of 0.04 g/L and a pH of 8.17 (Wu et al., 2014). The geology around the lake is dominated by Variscan biotite granite to the north. To the south Cambrian Ordovician sandstone and siltstone dominate, but Devonian tuff is also present (Feng, 1993). The climate of the Altay Mountains is primarily affected by a westerly airflow, which causes an average 45%–50% of the annual 700–900 mm of precipitation to occur between November and May (Zhang et al., 2015). The lake receives melt water from the Kanas glacier via the Kanas River, as well as from glaciers in the north via the Akuligun River, it also receives inflow from several ephemeral gullies. The outflow stream emerges from the southern part of the lake and flows into the Ergis River. According to historical records, flood is one of the most serious natural disasters in the Altay region, which has occurred frequently in the past 300 years, mainly manifested as snowmelt flood, rain-on-snow flood and rainstorm flood (Wen et al., 2006). Increasing snowmelt flood events in the spring and rainstorm flood events in the summer both occur as a consequence of the shift from a warm-dry to a warm-humid climate in northwest China (Shi et al., 2003, 2007), which has induced highly detrimental effects on the regional economy.

2.2 Data and processing

In August of 2012, an 82 cm long sediment core (KS) was retrieved from the south basin of Kanas Lake from

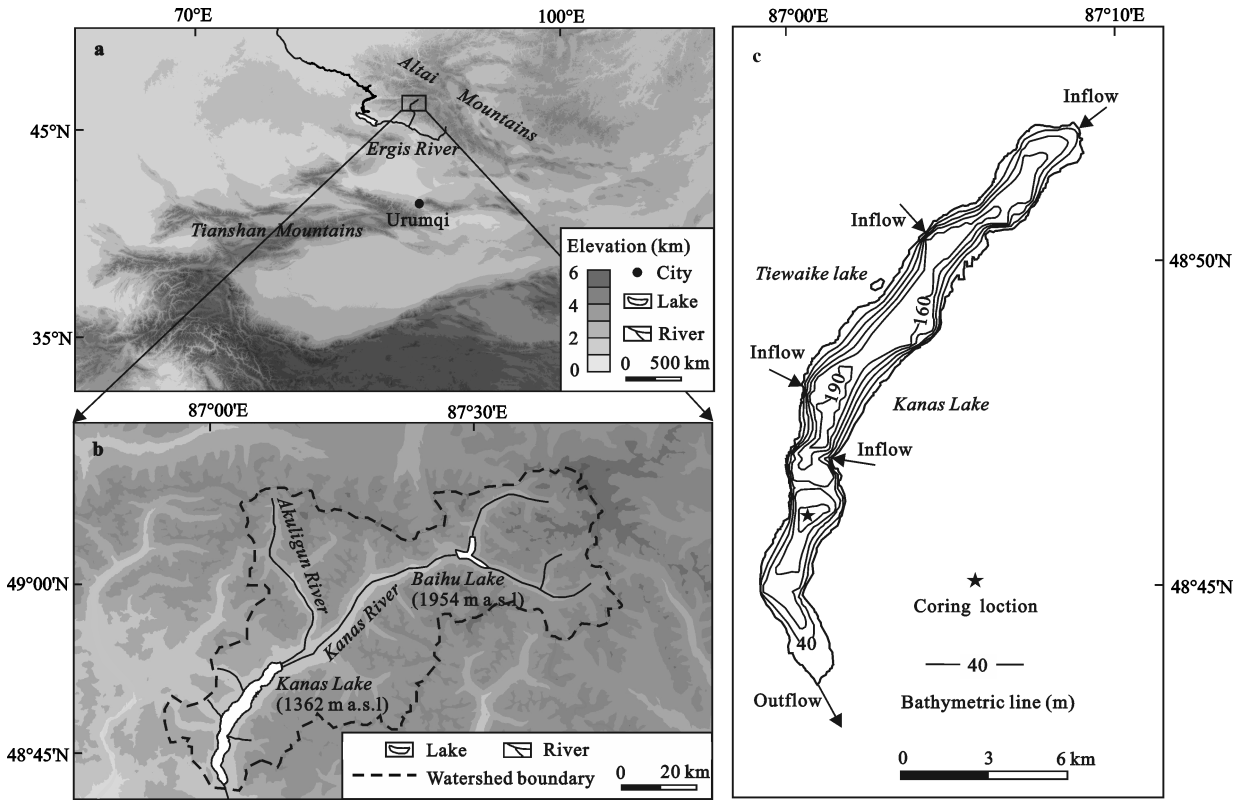

Fig. 1 Maps demonstrating the locations of Kanas Lake and the sediment core (KS). a) Geographic location of Kanas Lake. b) Watershed of Kanas Lake. c) Bathymetry of Kanas Lake and coring location

a water depth of ~170 m (Fig. 1c), using a gravity corer. The core for measurement of ^{210}Pb and ^{137}Cs was sampled at 0.5-cm interval to get a high resolution dating sequence, and the core for analysis of grain size was sectioned at 1-cm intervals in the laboratory. Samples were thereafter sealed in plastic bags and then stored in a freezer. This paper presents the results of the subsequent analysis of the layer sediments above a depth of 40 cm.

2.3 Methods

2.3.1 ^{210}Pb and ^{137}Cs dating

Sub-sample of dried sediment were analyzed for ^{210}Pb and ^{137}Cs through direct gamma spectrometry, using an Ortec HPGe GWL series, well-type, coaxial, low background, intrinsic germanium detector. ^{210}Pb activity was determined via gamma emissions of the samples at 46.5 keV, and ^{226}Ra activity by 295 and 352 keV γ-rays emitted by its daughter isotope ^{214}Pb, following 3 weeks of storage in sealed containers in order to allow for radioactive equilibration. ^{137}Cs was measured by its emissions at 662 keV. Supported ^{210}Pb activity within each sample was assumed to be in equilibrium with in situ ^{226}Ra activity. Unsupported ^{210}Pb activity (^{210}Pb$_{ex}$) at each depth was calculated by subtracting the ^{226}Ra activity from the total ^{210}Pb activity (^{210}Pb$_{tot}$).

In general, two basic models are available for age calculations based on ^{210}Pb activity: the constant of ^{210}Pb supply (constant rate of supply, CRS) model and the constant initial concentration of unsupported ^{210}Pb (^{210}Pb$_{ex}$) (constant initial concentration, CIC) model (Appleby and Oldfield, 1978). The CRS model assumes a constant supply of fallout ^{210}Pb irrespective of any changes in the sedimentation rate, while the CIC model assumes a constant initial concentration (Appleby, 2008). Because Kanas Lake is a water passing lake, the sedimentation rate might change with time, therefore we employed the CRS model to date the sediment core. The age of sediments at m depth (T_m) can be calculated by Eq. (1) with the CRS model:

$$T_m = T_0 - \ln(A_0 / A_m) / \lambda \quad (1)$$

where T_0 is the sampling year, λ is the decay constant (0.031 14/yr), A_0 is the total ^{210}Pb$_{ex}$ in the sediment core, and A_m is the total ^{210}Pb$_{ex}$ below m depth.

2.3.2 Grain size analysis

All samples were pretreated by adding 10% H_2O_2 to

remove organic matter and 10% HCL to remove carbonates, and were dispersed with 5% $(NaPO_3)_6$ with an ultrasonic treatment before the grain-size measurements. The grain-size distribution was measured by a Malvern Mastersizer 2000 laser diffraction instrument with 100 bins ranging from 0.02 to 2000 μm located at the State Key Laboratory of Lake Science and Environment, Nanjing Institute of Geography and Limnology, Chinese Academy of Science.

3 Results and Analyses

3.1 Lithology and chronology of sediment core

The KS core mainly consists of clay silt, although sandy silt is the major component in the layers between the depths of 35–32 cm and of 20–18 cm (Fig. 2). ^{210}Pb dating and ^{137}Cs dating were applied here to establish the age/depth relationship of the sediment core. Fig. 2a illustrates the vertical distribution of $^{210}Pb_{ex}$ and ^{137}Cs activities in the core. The $^{210}Pb_{ex}$ activity reaches equilibrium below a depth of 20 cm. Above a depth of 20-cm, $^{210}Pb_{ex}$ activity overall exhibits an approximately exponential decrease with an increasing depth in the core. The $^{210}Pb_{ex}$ activity within the core declined from 1254 Bq/kg at the core surface; to 80 Bq/kg at 6.5 cm; to 43 Bq/kg at 12.0 cm; to 16 Bq/kg at 17.0 cm and to nearly zero at 20.0 cm depth. The chronologies of ^{210}Pb were calculated using a CRS model (Appleby and Oldfield, 1978) and obtained 0.104 cm/a of average sedimentation rate for the interval 20–0 cm depth by fitting the average deposition rate of 20–0 cm with a least squares method ($s = -\lambda/a$, where s is the deposition rate, a is the slope of m and $\ln(^{210}Pb_{ex})$ at m depth, the $^{210}Pb_{ex}$ data was fitted by the exponential method). The ^{137}Cs activity shows a relatively well-resolved peak at 5 cm, which delineates the 1963 fallout maximum from atmospheric testing of nuclear weapons (Garcia-Orellana et al., 2006). The sedimentation rate calculated from the ^{137}Cs dates is 0.106 cm/a, which is very close to the sedimentation rate calculated from the $^{210}Pb_{ex}$ CRS model, therefore, the CRS model for core KS is robust. With this, based upon the CRS model, the dating sequence for the core was established. The ages of 20 to 0 cm were calculated by the CRS model and the 20-cm horizon was assigned an age of 1880 AD, and the 40-cm horizon was assigned an age of 1688 AD according to the average deposition rate 0.104 cm/a. Fig. 2b displays the age/depth relationships generated from the CRS model of ^{210}Pb.

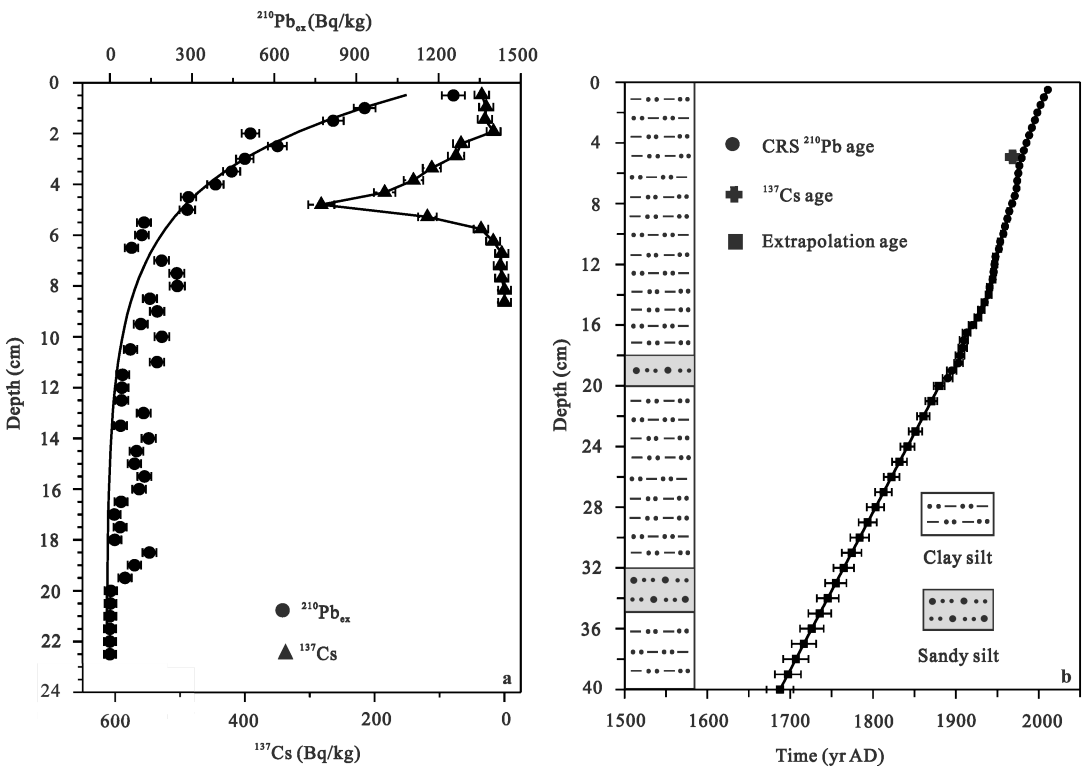

Fig. 2 Lithology and age model at Kanas Lake. a) The activities of ^{137}Cs and $^{210}Pb_{ex}$ versus depth in the sediment core from Kanas Lake. b) Age-depth relationship based on $^{210}Pb_{ex}$ and ^{137}Cs dating

3.2 Grain size

Grain-size parameters of lake sediments are sensitive to hydrodynamic conditions on an interannual to decadal scale (Chen et al., 2004). Consequently, interpretations regarding the hydrodynamic conditions and the related depositional processes can be drawn from various grain-size parameters. Different parameters of the grain-size distribution, including the median grain size (M_d), mean grain size (Mz), skewness (S_K), standard deviation (SD), kurtosis and contents of five size fractions (<4 μm, 4–16 μm, 16–32 μm, 32–63 μm, >63 μm) are shown in Fig. 3. Grain-size distributions within the sediment core are mainly composed of clay (<4 μm) and fine silt (4–16 μm), with respective contributions of 6.0%–52.9% and 11.0%–57.9%. The median silt (16–32 μm), coarse silt (32–63 μm), and sand (>63 μm) fractions account for 1.8%–19.5%, 0.4%–30.0% and 0–31.5% of the sediment, respectively. The Mz value ranges from 3.5 to 40.7 μm, the M_d value ranges from 3.8 to 46 μm, the SD value ranges from 1.2 to 2.2, the S_K value ranges from –0.14 to 0.42, and the kurtosis value ranges from 0.84 to 1.32. Down-core variations of all the grain-size parameters do not exhibit significant decreasing or increasing trends, but are characterized by two main periods (ca. 1736–1765 AD and ca. 1880–1905 AD), during which the contents of the 16–32 μm, 32–63 μm, and >63 μm size fractions, as well as the values of Mz and M_d significantly increased, while the contents of the <4 μm and 4–16 μm size fractions decreased significantly. During these two periods, the M_d values and the content of the >63 μm size fraction exhibited the clearest signal. From 1736 AD to 1765 AD, the content of the >63 μm size fraction increased sharply to a maximum peak of 35%, and the M_d values also increased sharply to a maximum peak of 46 μm. Between 1880 and 1905 AD, the content of the >63 μm size fraction increased to a secondary peak of 30.4%, and the M_d values also increased to a secondary peak of 23.3 μm. The values of S_K and SD also rose during these two periods, but in a different fashion than the other grain-size parameters, suggesting that these two periods are not the only two timespans with peak values for S_K and SD.

Compared with the characteristics of the grain-size parameters, the frequency distribution curves can directly reflect the grain-size population (i.e., as uni-modal or poly-modal). The size range and proportion of each grain-size population can be calculated and subsequently utilized to deduce the material source and transport pattern of the corresponding grain-size population. Fig. 4a displays the frequency distributions for the sediment core at different depths. The frequency distributions for Kanas Lake sediment core primarily include two apparent grain-size populations, and the proportions of which vary with depth. One grain-size population has a prominent peak centered at 3–9 μm, and was abundant in the core sediments, thus, it can be regarded as background sediments (Fig. 4b). The other population has a prominent peak centered at 40–100 μm, and was only

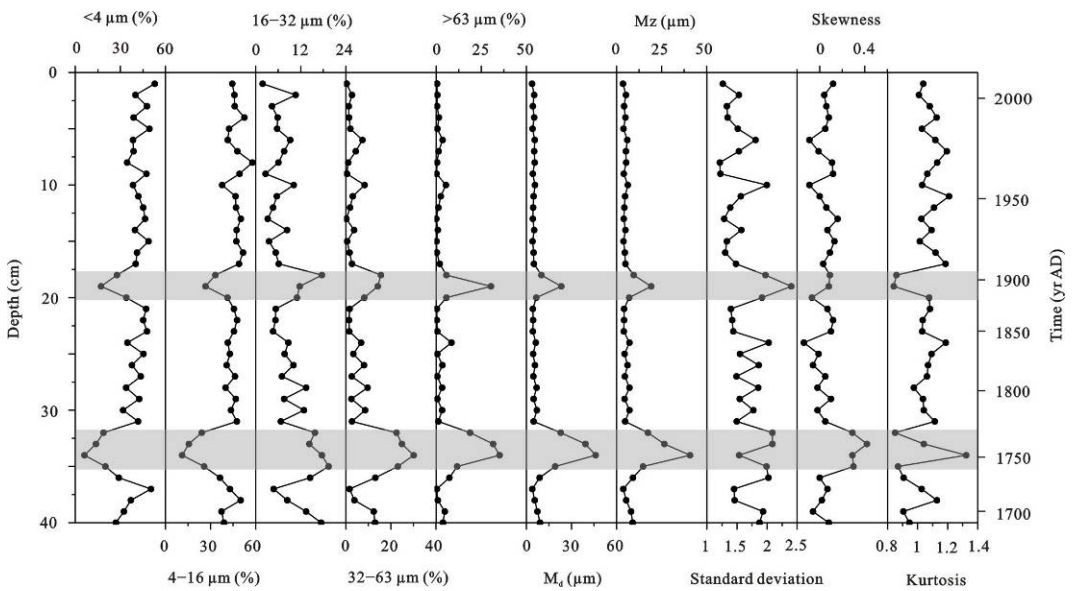

Fig. 3 Grain size distribution, standard deviation, and kurtosis of Kanas Lake sediment core. Mz is mean grain size

distributed in two layers, i.e., 35–32 cm and 20–18 cm in depth (corresponding to ca. 1736–1765 AD and ca. 1880–1905 AD, respectively). The frequency distributions for the 35–32 cm depth population has a pronounced peak centered at 40–100 μm (Fig. 4c), indicating that the sedimentary materials were derived primarily from a single source concordant with an increase in transport energy. The frequency distributions for the 20–18 cm depth population possesses flat bimodal curves with two peaks centered at 3–9 μm and 40–100 μm, respectively (Fig. 4d). The two similar bimodal profiles indicate that the sedimentary materials may have been transported from different sources. In summary, the sedimentary environment during these two periods changed significantly.

4 Discussion

The grain-size parameters of Kanas Lake sedimentary core demonstrate two abrupt environment shifts corresponding to ca. 1736–1765 AD and ca. 1880–1905 AD, respectively. The frequency distributions for these two periods are marked with a prominent peak centered at 40–100 μm (Figs. 4c, 4d). During ca. 1736–1765 AD, the frequency distributions of Kanas Lake sediments exhibit a uni-modal distribution, and are comparable to that of typical sediments that were deposited under a strong hydrodynamic condition (Fig. 4c) (Yin et al., 2008), similar to the frequency distributions of flood layers from Oeschinen Lake situated in the north-western Alps (Fig. 4c) (Amann et al., 2015). This indicates that the uni-modal distribution of Kanas Lake sediments deposited during this period might have reflected flood events. However, during the period from ca. 1880–1905 AD, in addition to the 40–100 μm fraction, another minor peak exists that is centered at 3–9 μm. The bi-modal distribution of Kanas Lake sediments is similar to that of typical sediments that were deposited in a relatively unstable environment (Fig. 4d) (Yin et al., 2008), similar to flood deposits of the Dead Sea (Fig. 4d) (López-Merino et al., 2016). López-Merino et al. (2016) hypothesized that the bi-modal distribution of Dead Sea

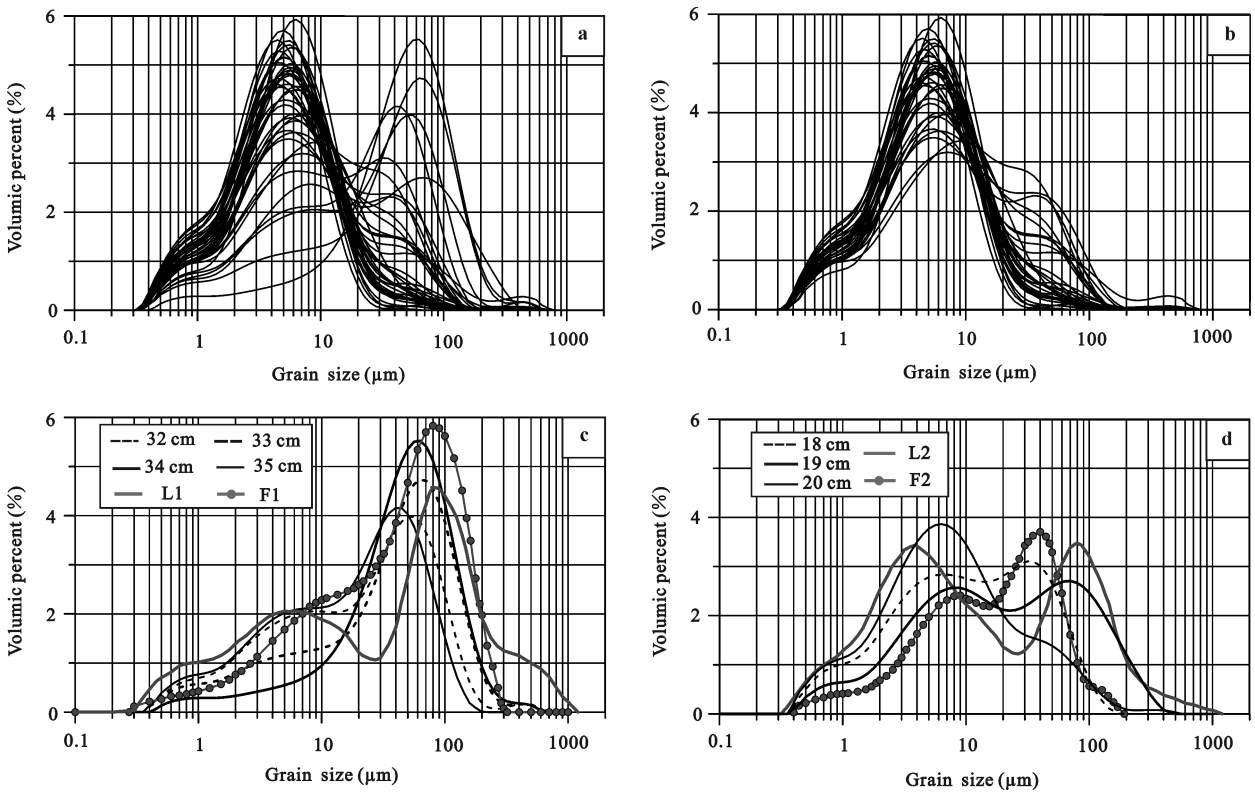

Fig. 4 The frequency distribution curves. a) Volumic percent of each grain-size class for all sediments. b) Volumic percent of each grain-size class for background sediments. c) Volumic percent of each grain-size class for the layer between 35–32 cm depth, L1 represents typical lakeshore sediments (Yin et al., 2008), and F1 represents a flood deposit from an alpine lake (Amann et al., 2015). d) Volumic percent of each grain-size class for the layer between 20–18 cm depth, L2 represents typical lake transition zone deposits (Yin et al., 2008), and F2 represents a flood deposit from the Dead Sea (López-Merino et al., 2016)

sediments, which were deposited during flood events, reflects two different sources, i.e., long-range transported dust (3–10 μm) and local run-off products from the catchment area (20–90 μm). The same applies to Kanas Lake, and thus, the bi-modal distribution of Kanas Lake sediments deposited at this time might also reflect flood events.

To further clarify the abrupt environmental events that were recorded in the sedimentary core of Kanas Lake from ca. 1736–1765 AD and ca. 1880–1905 AD, a statistical method known as canonical discriminant analysis (CDA) was applied here. CDA is a multivariate technique which can be used to determine the relationships among a categorical variable, thereby helping to separate groups in a lower-dimensional discriminant space (canonical space). When the sensitive grain size parameters were applied, the CDA was an effective method to differentiate between sedimentary environments that were closely related to the hydrodynamic force (Purkait and Majumdar, 2014). A total of six variables of the sediment grain parameters were used for CDA, including the mean grain size, skewness, standard deviation, kurtosis, Q90 (90th percentile) and Q10 (10th percentile). Squared Mahalanobis distances (d^2) were calculated to identify the distinctiveness among the different sedimentary environments. Two groups were distinctly separated within a lower-dimensional discriminant space according to their d^2 values (Fig. 5a). Clarification results indicate that group 2 is completely distinct from group 1 in terms of hydrodynamic conditions, which is a consequence of the larger d^2 values. Group 2 represents layers that were deposited during ca. 1736–1765 AD and ca. 1890 AD, while group 1 represents background sediments. Therefore, the two periods possessing strong hydrodynamic conditions, i.e., ca. 1736–1765 AD and ca. 1890 AD, were identified using the CDA method. In other words, two extreme hydrological events might have occurred during these two periods, although the characteristics and nature of either event are unclear.

C-M diagrams are widely utilized to distinguish between flood deposits and other coarse-grained deposits, since different sedimentary facies can be distinguished according to the C (90th percentile or Q90) and M (50th percentile or Q50) distributions, respectively (Wihelm et al., 2012; Arnaud et al., 2016). For example, ancient flood events recorded in sedimentary cores from Blanc Lake were identified based on the C-M pattern analysis (Wihelm et al., 2012). Two facies in the sediments from Kanas Lake were separated based upon the C-M pattern analysis (Fig. 5b). Facies 1 represents background sediments, while facies 2 represents layers that were deposited during ca. 1736–1765 AD and ca. 1890 AD. The well-restrained field for facies 1 in the diagram indicates a 'pelagic suspension' sedimentary deposit type. The well-sorted facies 2, as well as the parallelism within the facies 2 pattern and the Q90 = Q50 line (Fig. 5b), both suggest that these sediments have been sorted by a river transport process. This type of parallel relationship can be regarded as the signal of a flood event (Wihelm et al., 2012). Accordingly, layers deposited during ca. 1736–1765 AD and ca. 1890 AD can be considered as two flood event layers, which is in accordance

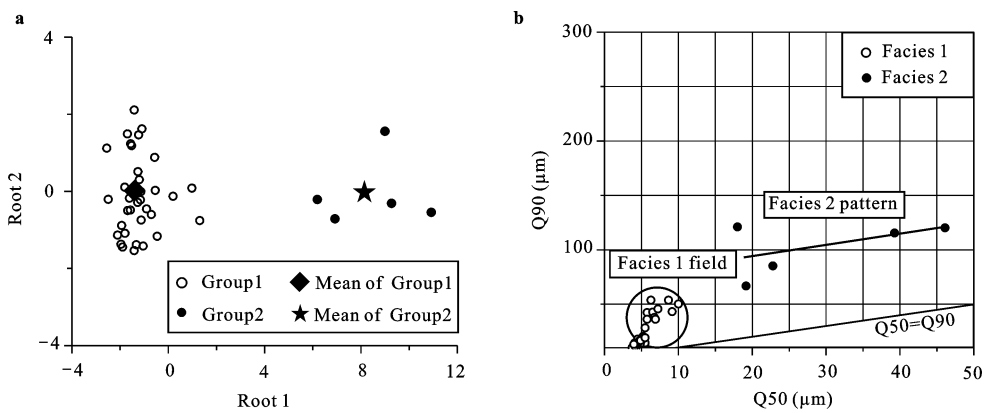

Fig. 5 Distinct properties between flood layers and the rest of the layers. a) Results of canonical discriminant analysis (CDA). The canonical score plot shows how the two canonical functions classify the observations between groups by plotting the observation score for each sample. b) Coarse percentile vs median grain size (C-M) pattern of Kanas Lake sediments. Facies 2 represents sandy silt, which is distributed in layers between 35–32 cm and 19 cm depth, while facies 1 represents clay silt, which is distributed throughout the rest of the layers.

with the results of CDA.

The frequency distributions and statistical analyses of grain-size parameters of Kanas Lake sedimentary core demonstrate that, over the past 300 years, Kanas Lake sediments may have recorded two extreme flood events in the Altay Mountain region, corresponding to ca. 1736–1765 AD and ca. 1890 AD. According to the present-day observed data, floods in the Altay Mountain area are mainly triggered by snowmelt and/or summer precipitation, and can be divided into three flood types, i.e., snowmelt floods, rain-on-snow floods and rainstorm floods (Nuerlan and Shen, 2014). For example, in June of 2010, under the influence of higher summer temperatures and heavier winter snowfall, a rain-on-snow flooding event occurred in the Altay region. Another flooding event, a rainstorm flood, characterized by less winter snowfall and more summer precipitation in June, occurred in 2012. Generally, winter snowfall, summer temperatures and summer precipitation are the three major factors in the triggering of flood events in the Altay area. During ca. 1736–1765 AD, corresponding to the first flooding event observed within the sedimentary core, the climate conditions were dominated by heavier and longer winter snowfall, with as much as 20 snow cover days more than the average value (115 days) in winter for this period, and about 0.3℃ higher summer temperatures than the average value (18.7℃) during the study period on the basis of tree-ring records in the Altay area (Zhang et al., 2008a; 2010), and temperatures rose drastically during the early summer in this period (Hu et al., 2012). In approximately 1890 AD, there was a positive abnormal value of about 0.25℃ and as much as 120 mm summer precipitation higher than the average value (260 mm) during the study period according to tree-ring records from the Altay region (Zhang et al, 2008a; 2008b), the climate condition was characterized by higher summer temperatures and heavier summer precipitation, which probably triggered the flood event in this period. In summary, both of these two flood events occurred during warmer and wetter climate conditions. Higher temperatures are likely to strengthen convective conditions, resulting in an increase in the intensity of precipitation events and hence enhancing flood intensity (Wihelm et al., 2013), while wet conditions are always accompanied by more summer precipitation and winter snowfall, thus increasing the flood frequency. Such a relationship between flood intensity and frequency, temperature and precipitation peaks has been deduced in the Alps mountain regions (Wihelm et al., 2012; 2013). These two flood event periods were the two main temperature-increasing stages during 18th and 19th centuries according to the reconstruction of the extra-tropical North Hemisphere mean temperature (Christiansen and Ljungqvist, 2012), thereby triggering these flood events over a 300-year period to a great extent. Moreover, the flood events in Kanas Lake sedimentary record also existed in the adjacent regions. Li et al. (2016) reported two flood events in ca. 1760 AD and ca. 1880 AD within the sedimentary record of Tiewaike Lake, which is relatively close to Kanas Lake. By estimating grain-size parameters in the sediments of Bosten Lake, Huang et al. (2008) suggested that flood events might have also occurred in those two periods in Bosten Lake of the southern Tianshan Mountains. Similar events might have been also recorded by the sediments in Balkhash Lake in the western Tianshan Mountains during ca. 1600–1780 AD and ca. 1840–1950 AD, since the rainfall increased within the Balkhash Lake region during these two periods (Chiba et al., 2016).

According to a comparative analysis between our sedimentary flood records and tree-ring records, the two extreme flood events in the Altay area both occurred during warmer and wetter climate conditions. Such climate characteristics were widely distributed during these two periods, in particular, the wetter conditions appear to have persisted in large areas throughout ACA during ca. 1736–1765 AD. For example, a reconstruction of the Selenga River streamflow in west-central Mongolia verifies that the period from 1764 AD to 1768 AD represents the wettest period during the past millennium (Davi et al., 2006). Observations from Chen et al. (2010) in the Badain Jaran desert indicated that the groundwater recharge rates, which were obtained from a reconstruction using the chloride mass balance in the unsaturated zone, were extremely high around 1750 AD, suggesting a humid climate during this period. A relatively wet period from the 1740s to 1780s was also reported for the central Tianshan region according to the tree-ring record (Li et al., 2006). Based on interpretations of multiple climatic proxies of the Aral Sea, the climate of the Aral Sea area was warmer and wetter during the period from 1650 AD to 1780 AD (Boomer et al., 2009). All this evidence suggests that humid climatic conditions existed broadly across the ACA during this

period. At present, precipitation in ACA regions is primarily the product of the transportation of depressions into continental regions, as well as cyclone storms that initially formed over the eastern Mediterranean, by a westerly jet stream (Chen et al., 2010). Moreover, a humid climate in those regions always correlates with the successful penetration of depressions into ACA, and the shifting of storms tracks farther south during a negative NAO phase (Aizen et al., 1997). This mechanism also applies to rainfall in the surrounding high mountains in northwestern China (Chen et al., 2010). During ca. 1736–1765 AD, the NAO existed in a negative phase (Trouet et al., 2009), during which period the axis of maximum moisture transport, as well as of cyclonic storm tracks, shifted southward, resulting in increased precipitation in the study region. This may have triggered extreme flood events in the Altay and Tianshan Mountains. This finding is also concurrent with higher flood frequencies around 1740 AD in the Alpine Mountain area (Glur et al., 2013), since the Alps are also located along the trajectory of westerly transport.

Generally speaking, it is difficult to access the relationship between flood events and climate change because of the lack of long-term meteorological data at high altitudes. Furthermore, the stochastic nature of extreme events preclude the identification of long-term trends, yet two extreme flood events in the Altay mountain region have been identified by grain-size parameters analysis of Kanas Lake sediments, both of which occurred in a warmer and wetter climate condition. Although it is not straightforward to elaborate the feedback mechanism between flood events and climate conditions based on Kanas Lake record, the apparent link between high intensity floods and warmer, wetter climate condition provides motivation for further deliberations. Accepting that extreme floods are triggered by warmer and wetter climate condition suggests that more extreme flood events will occur in a world undergoing global warming. Our study thus provides important evidence that warming may play an important role in flood activity, favoring an increase in flood intensity and flood frequency on a multi-decennial time scale. However, this conjecture needs to be further tested by more flood records from mountain lakes in arid regions.

5 Conclusions

The grain size data of a sediment core (KS) in Kanas Lake was used to reconstruct a flood history over the past 300 years within the Altay Mountains, northwestern China. Both grain-size parameters and frequency distributions demonstrate two abrupt environmental events. Moreover, by applying CDA and C-M pattern analysis, two extreme flood events corresponding to ca. 1736–1765 AD and ca. 1890 AD were identified. Combined with tree-ring records, these events occurred during warmer and wetter climate conditions, indicating that flood intensity and frequency may increase during a potential future warmer and wetter climate in northwestern China. In addition, a comparison with other records from adjacent regions shows that these two flood events existed elsewhere, especially the first flooding event, which appears to have existed in large areas of ACA. This event may have also extended farther towards the west within the European Alps, a correlation that appears to be associated with changes in the NAO index.

Acknowledgements

We would like to thank MA Long and Kanas Scenic Spot Management Committee for their field assistances.

References

Aizen V B, Aizen E M, Melack J M et al., 1997. Climate and hydrologic change in the Tien Shan, Central Asia. *Journal of Climate*, 10(6): 1393–140. doi: 10.1175/1520-0442(1997)010<1393:CAHCIT>2.0.CO;2

Amann B, Szidat S, Grosjean M, 2015. A millennial-long record of warm season precipitation and flood frequency for the North-western Alps inferred from varved lake sediments: implications for the future. *Quaternary Science Reviews*, 115: 89–100. doi: 10.1016/j.quascirev.2015.03.002

Appleby P G, Oldfield F, 1978. The calculation of lead-210 dates assuming a constant rate of supply of unsupported ^{210}Pb to the sediment. *Catena*, 5(1): 1–8. doi: 10.1016/S0341-8162(78)80002-2

Appleby P G, 2008. Three decades of dating recent sediments by fallout radionuclides: a review. *The Holocene*, 18(1): 83–93. doi: 10.1177/0959683607085598

Arnaud F, Poulenard J, Giguet-Covex C et al., 2016. Erosion under climate and human pressures: an alpine lake sediment perspective. *Quaternary Science Reviews*, 152: 1–18. doi: 10.1016/j.quascirev.2016.09.018

Boomer I, Wünnemann B, Mackay A W et al., 2009. Advances in understanding the late Holocene history of the Aral Sea region. *Quaternary International*, 194(1): 79–90. doi: 10.1016/j.quaint.2008.03.007

Chen F H, Chen J H, Holmes J et al., 2010. Moisture changes over the last millennium in arid central Asia: a review, synthesis and comparison with monsoon region. *Quaternary Science Reviews*, 29(7–8): 1055–1068. doi: 10.1016/j.quascirev.2010.01.005

Chen Jingan, Wan Guoqiang, Zhang D D et al., 2004. Environmental records of lacustrine sediments in different time scales: Sediment grain size as an example. *Science in China: Series D: Earth Sciences*, 47(10): 954–960. doi: 10.1360/03yd0160

Chen J H, Chen F H, Feng S et al., 2015. Hydroclimatic changes in China and surroundings during the Medieval Climate Anomaly and Little Ice Age: spatial patterns and possible mechanisms. *Quaternary Science Reviews*, 107: 98–111. doi: 10.1016/j.quascirev.2014.10.012

Chiba T, Endo K, Sugai T et al., 2016. Reconstruction of Lake Balkhash levels and precipitation/evaporation changes during the last 2000 years from fossil diatom assemblages. *Quaternary International*, 397: 330–341. doi: 10.1016/j.quaint.2015.08.009

Christiansen B, Ljungqvist F C, 2012. The extra-tropical Northern Hemisphere temperature in the last two millennia: reconstructions of low-frequency variability. *Climate of the Past*, 8(2): 765–786. doi: 10.5194/cp-8-765-2012

Corella J P, Benito G, Rodriguez-Lloveras X et al., 2014. Annually-resolved lake record of extreme hydro-meteorological events since AD 1347 in NE Iberian Peninsula. *Quaternary Science Reviews*, 93: 77–90. doi: 10.1016/j.quascirev.2014.03.020

Davi N K, Jacoby G C, Curtis A E et al., 2006. Extension of Drought Records for Central Asia Using Tree Rings: west-central Mongolia. *Journal of Climate*, 19(2): 288–299. doi: 10.1175/JCLI3621.1

Easterling D R, Meehl G A, Parmesan C et al., 2000. Climate extremes: observations, modeling, and impacts. *Science*, 289(5487): 2068–2074. doi: 10.1126/science.29.5487.2068

Feng Min, 1993. Landform and origin of Hanas Lake, Altay Mountains. *Journal of Glaciology and Geocryology,* 15(4): 559–565. (in Chinese)

Garcia-Orellana J, Sanchez-Cabeza JA, Masqué P et al., 2006. Atmospheric fluxes of ^{210}Pb to the western Mediterranean Sea and the Saharan dust influence. *Journal of Geophysical Research: Atmospheres*, 111(D15): D15305. doi: 10.1029/2005JD006660

Glur L, Wirth S B, Büntgen U et al., 2013. Frequent floods in the European Alps coincide with cooler periods of the past 2500 years. *Scientific Reports*, 3: 2770. doi: 10.1038/srep02770

Hu Yicheng, Yuan Yujiang, Wei Weishou et al., 2012. Tree-ring reconstruction of mean June–July temperature during 1613–2006 in east Altay, Xinjiang of China. *Journal of Desert Research*, 32(4): 1003–1009. (in Chinese)

Huang Xiaozhong, Chen Fahu, Xiao Sun et al., 2008. Primary study on the environmental significances of grain-size changes of the Lake Bosten sediments. *Journal of Lake Sciences*, 20(3): 291–297. doi: 10.18307/2008.0305. (in Chinese)

IPCC, 2013. Climate change 2013: the physical science basis. In: Stocker T F et al. (eds). *Contribution of Working Group I to the Fifth Assessment Report of the Intergovernmental Panel on Climate Change*. Cambridge, United Kingdom and New York, NY, USA: Cambridge University Press.

Li J B, Gou X H, Cook E R et al., 2006. Tree-ring based drought reconstruction for the central Tien Shan area in northwest China. *Geophysical Research Letters*, 33(7): L07715. doi: 10.1029/2006GL025803

Li Y F, Guo Y, Yu G. 2013. An analysis of extreme flood events during the past 400 years at Taihu lake, China. *Journal of Hydrology*, 500: 217–225. doi: 10.1016/j.jhydrol.2013.02.028

Li Y, Qiang M R, Zhang J W et al., 2016. Hydroclimatic changes over the past 900 years documented by the sediments of Tiewaike Lake, Altai Mountains, northwestern China. *Quaternary International*, 452: 91–101. doi: 10.1016/j.quaint.2016.07.053

Liu C T, Zipser E J, 2015. The global distribution of largest, deepest, and most intense precipitation systems. *Geophysical Research Letters*, 42(9): 3591–3595. doi: 10.1002/2015GL063776

López-Merino L, Leroy S A G, Eshel A et al., 2016. Using palynology to re-assess the Dead Sea laminated sediments: indeed varves? *Quaternary Science Reviews*, 140: 49–66. doi: 10.1016/j.quascirev.2016.03.024

Ma L, Wu J L, Abuduwaili J et al., 2015. Aeolian particle transport inferred using a ~150-year sediment record from Sayram Lake, arid northwest China. *Journal of Limnology*, 74(3): 584–593. doi: 10.4081/jlimnol.2015.1208

Min S K, Zhang X B, Zwiers F W et al., 2011. Human contribution to more-intense precipitation extremes. *Nature*, 470(7334): 378–381. doi: 10.1038/nature09763

Nuerlan Hazaizi, Shen Yongping, 2014. Flood characteristics of Altay area, Xinjiang. *Journal of China Hydrology*, 34(4): 74–81. (in Chinese)

Oldfield F, 2005. *Environmental Change: Key Issues and Alternative Approaches.* Cambridge, UK: Cambridge University Press.

Pall P, Aina T, Stone D A et al., 2011. Anthropogenic greenhouse gas contribution to flood risk in England and Wales in autumn 2000. *Nature*, 470(7334): 382–385. doi: 10.1038/nature09762

Purkait B, Majumdar D D, 2014. Distinguishing different sedimentary facies in a deltaic system. *Sedimentary Geology*, 308(7): 53–62. doi: 10.1016/j.sedgeo.2014.05.001

Schillereff D N, Chiverrell R C, Macdonald N et al., 2014. Flood stratigraphies in lake sediments: a review. *Earth-Science Reviews*, 135: 17–37. doi: 10.1016/j.earscirev.2014.03.011

Shi Yafeng, Shen Yongping, Li Dongliang et al., 2003. Discussion on the present climate change from warm-dry to warm-wet in northwest china. *Quaternary Sciences*, 23(2): 152–164. (in Chinese)

Shi Y F, Shen Y K, Kang E S et al., 2007. Recent and Future Climate Change in Northwest China. *Climatic Change*, 80(3–4): 379–393. doi: 10.1007/s10584-006-9121-7

Trouet V, Esper J, Graham N E et al., 2009. Persistent positive North Atlantic oscillation mode dominated the medieval cli-

mate anomaly. *Science,* 324(5923): 78-80. doi: 10.1126/science.1166349

Wang Hao, Liu Guohua, Li Zongshan et al., 2016. Impacts of Climate Change on Net Primary Productivity in Arid and Semiarid Regions of China. *Chinese Geographical Science*, 26(1): 35–47. doi: 10.1007/s11769-015-0762-1

Wen Kegang, Shi Yuguang, 2006. *China Meteorological Disasters Books: Xinjiang Volume*. Beijing: China Meteorological Press, 75–146. (in Chinese)

Wilhelm B, Arnaud F, Enters D et al., 2012. Does global warming favour the occurrence of extreme floods in European Alps? First evidences from a NW Alps proglacial lake sediment record. *Climatic Change*, 113(3–4): 563–581. doi: 10.1007/s10584-011-0376-2

Wilhelm B, Arnaud F, Sabatier P et al., 2013. Palaeoflood activity and climate change over the last 1400 years recorded by lake sediments in the north-west European Alps. *Journal of Quaternary Science*, 28(2): 189–199. doi: 10.1002/jqs.2609

Wu J L, Liu W, Zeng H A et al., 2014. Water Quantity and Quality of Six Lakes in the Arid Xinjiang Region, NW China. *Environmental Processes*, 1(2): 115–125. doi: 10.1007/s40710-014-0007-9

Xiao J L, Chang Z G, Wen R L et al., 2009. Holocene weak monsoon intervals indicated by low lake levels at Hulun Lake in the monsoonal margin region of northeastern Inner Mongolia, China. *The Holocene*, 19(6): 899–908. doi: 10.1177/0959683609336574

Yin Zhiqiang, Qin Xiaoguang, Wu Jinshui et al., 2008. Multimodal grain-size distribution characteristics and formation mechanism of lake sediments. *Quaternary Sciences*, 28(2): 345–353. (in Chinese)

Zhang M, Chen Y N, Shen Y J et al., 2017. Changes of precipitation extremes in arid Central Asia. *Quaternary International,* 436: 16–27. doi:10.1016/j.quaint.2016.12.024

Zhang Tongwen, Yuan Yujiang, Yu Shulong et al., 2008a. Reconstructed mean temperature series from May to September with tree-ring in the western region of Altay near the recent 365 a. *Arid Zone Research*, 25(2): 288–294. (in Chinese)

Zhang Tongwen, Yuan Yujiang, Yu Shulong et al., 2008b. June to September precipitation series of 1481–2004 reconstructed from tree-ring in the western region of Altay Prefecture, Xinjiang. *Journal of Glaciology and Geocryology*, 30(4): 659–657. (in Chinese)

Zhang Tongwen, Yuan Yujiang, Wei Wenshou et al., 2010. Reconstructed number of snow cover depth ≥0 cm days changes in the western Altai Prefecture, using tree-ring width chronologies. *Desert and Oasis Meteorology*, 4(3): 6–11. (in Chinese)

Zhang Wei, Fu Yanjing, Liu Beibei et al., 2015. Geomorphological process of late Quaternary glaciers in Kanas river valley of the Altay Mountains. *Acta Geographic Sinica*, 70(5): 739–750. (in Chinese)